Published in final edited form as:

Am J Med Genet A. 2018 June ; 176(6): 1443–1448. doi:10.1002/ajmg.a.38717.

Mutations in *SZT2* result in early-onset epileptic encephalopathy and leukoencephalopathy

Amy Pizzino[1], **Matthew Whitehead**[2,3], **Parisa Sabet Rasekh**[1], **Jennifer Murphy**[4], **Guy Helman**[5], **Miriam Bloom**[6], **Sarah H. Evans**[1], **John G. Murnick**[3], **Joan Conry**[1], **Ryan J. Taft**[4,7], **Cas Simons**[4], **Adeline Vanderver**[1,8,9,10], **Laura A. Adang**[10]

[1]Department of Neurology, Children's National Medical Center, Washington, DC [2]Department of Neuroradiology, The George Washington University School of Medicine, Washington, DC [3]Department of Diagnostic Imaging and Radiology, Children's National Medical Center, Washington, DC [4]Undiagnosed Disease Program, National Human Genome Research Institute (NHGRI), Bethesda, Maryland [5]Institute for Molecular Bioscience, University of Queensland, St. Lucia, Queensland, Australia [6]Department of Pediatrics, Children's National Medical Center, Washington, DC [7]Illumina, Inc., San Diego, California [8]Center for Genetic Medicine Research, Children's National Medical Center, Washington, DC [9]School of Medicine and Health Sciences, George Washington University, Washington, DC [10]Division of Neurology, Children's Hospital of Philadelphia, Philadelphia, Pennsylvania

Abstract

Early-onset epileptic encephalopathies (EOEEs) are a genetically heterogeneous collection of severe epilepsies often associated with psychomotor regression. Mutations in *SZT2,* a known seizure threshold regulator gene, are a newly identified cause of EOEE. We present an individual with EOEE, macrocephaly, and developmental regression with compound heterozygous mutations in *SZT2* as identified by whole exome sequencing. Serial imaging characterized the novel finding of progressive loss of central myelination. This case expands our clinical understanding of the *SZT2*-phenotype and emphasizes the role of this gene in the diagnostic investigation for EOEE and leukoencephalopathies.

Keywords

early-onset epileptic encephalopathy; leukoencephalopathy; myelination; SZT2; whole exome sequencing

Correspondence: Laura A. Adang, Division of Neurology, Children's Hospital of Philadelphia, Philadelphia, PA., adangl@email.chop.edu.

CONFLICT OF INTEREST

None.

1 | INTRODUCTION

Early-onset epileptic encephalopathies (EOEEs) are a group of genetically heterogeneous epilepsies in children and are typically associated with psychomotor regression. As recently described, mutations in *SZT2,* a known seizure threshold regulator gene, are a rare cause of EOEE (Basel-Vanagaite et al., 2013; Falcone et al., 2013; Nakamura et al., 2017; Tshuchida et al., 2017; Venkatesan, Angle, & Millichap, 2016). Highly expressed in the central nervous system, SZT2 is associated with the regulation of mammalian target of rapamycin (mTOR) and epileptogenesis in humans and animal models (Baldassari, Licchetta, Tinuper, Bisulli, & Pippucci, 2016; Frankel, Yang, Mahaffey, Beyer, & O'Brien, 2009; Peng, Yin, & Li, 2017; Toutzaris et al., 2010). It is theorized that dysfunctional Szt2 inhibits the suppression of mTOR (Baldassari et al., 2016; Peng et al., 2017; Wolfson et al., 2017).

Prior clinical reports have described the role of *SZT2* in refractory epilepsy and intellectual disability. Reported imaging findings include atrophy and dysgenesis of the corpus callosum (Table 1) (Basel-Vanagaite et al., 2013; Falcone et al., 2013; Nakamura et al., 2017; Tshuchida et al., 2017; Venkatesan et al., 2016). In this context, we will review the existing literature and present the case of an affected child with compound heterozygous variants in *SZT2* and EOEE with the novel finding of loss of central myelination (Table 1).

2 | CLINICAL REPORT

The proband is a girl who presented to medical attention with seizures at 20 months of age. Her neurologic examination was notable for macrocephaly (head circumference 51 cm, >2 standard deviations above norm), dysmorphic features (frontal bossing, hypertelorism, microophthalmia, depressed nasal bridge, long-tapered fingers, and hyper-extensible joints), global hypotonia, and intact deep tendon reflexes. Developmentally, she sat independently at 15 months and pulled to a stand at 40 months. She never produced specific words, and her receptive language skills were limited. Her encephalopathy was progressive and, by the age of 7, she had lost the ability to communicate, purposefully use her limbs, and was gastrostomy tube dependent. Her later examinations were notable for diffuse alopecia and rashes, choreoathetosis, and areflexia. She died at 8 years of age following a prolonged hospital course, complicated by syndrome of inappropriate antidiuretic hormone (SIADH), chronic pancreatitis, and sepsis. A three-generation pedigree was significant for maternal relatives with developmental delay of unknown etiology, although neither parent was affected.

Her electroencephalogram was characterized by multifocal epileptiform discharges. She had frequent focal motor seizures with impaired consciousness arising from both hemispheres with intermittent evolution into bilateral convulsive seizures. Her epilepsy was refractory to multiple medications, including lamotrigine, levetiracetam, phenytoin, phenobarbital, topiramate, rufinamide, midazolam, and the ketogenic diet.

3 | NEUROIMAGING

Brain magnetic resonance imaging (MRI) exams were performed on either a 1.5T or 3T magnet (General Electric, Milwaukee, WI). Sagittal T1WI, axial T2WI, coronal T2WI,

coronal or axial gradient echo, and axial diffusion weighted images were performed in all cases. Axial proton density (<1 year) or T2 FLAIR images (>1 year) were also obtained in accordance with age. Post contrast coronal and axial T1WI were performed in three exams after intravenous injection of 0.1 mmol/kg gadopentetate dimeglumine. Single voxel magnetic resonance spectroscopy (MRS) was performed with a 2 × 2 × 2 cm voxel of interest over the left basal ganglia in three exams (TR 2000 ms, TE 288 ms).

The initial brain MRI at 11 months of age demonstrated megalencephaly with an increased fronto-occipital diameter and thickened corpus callosum for age (Figure 1[1a,b]). Midline anomalies included absence of the thalamic massa intermedia and blunting of the rostrum, consistent with callosal dysgenesis (Figure 1[1a]). Myelination was age appropriate at this time. No significant change occurred in the interim between this exam and a follow-up brain MRI at 21 months of life (Figure 1[2a,b]). However, MRS revealed low creatine (Figure 1[2c]).

By 31 months, mild diffuse brain volume loss and hypomyelination had developed (Figure 1[3a–c]). Creatine depression was less pronounced (Figure 1[3d]). Follow-up exams at 3 years (Figure 1[4]), 4 years (Figure 1[5]), and 7 years (Figure 1[6]) show further regression of myelination and progressive diffuse brain volume loss with eventual development of abnormal signal in the splenium (Figure 1[5,6]). By age 4, the adenohypophysis is mildly enlarged (Figure 1[5a]), with increasing size and loss of normal posterior pituitary signal on follow-up MRI at age 7 (Figure 1[6a]). Hypertelorism and symmetric mild microphthalmia is noted on orbital images (Figure 1[6d]).

4 | MOLECULAR ANALYSES

The patient was prospectively enrolled in the Myelin Disorders Bioregistry Project study of Unclassified Leukoencephalopathies at Children’s National Medical Center. Triplet whole exome sequencing (WES) of DNA was performed at the Queensland Centre for Medical Genomics using the Illumina Nextera Rapid Capture kit, and captured libraries were sequenced on an Illumina HiSeq 2000 (2 × 100 nt). Each exome was sequenced to a minimum depth such that 90% of targeted bases were sequenced to a read depth of ≥20× (average 92%). Reads were aligned to the reference human genome (GRCh37) and pedigree informed variant calling was performed using the Real Time Genomics integrated analysis tool rtgFamily v3.2 (Cleary et al., 2014). All variants were annotated using SnpEff v4.2 and filtered using data from the SnpEff GRCh37.75 database, dbSNP147, and dbNSFP v2.9 (Cingolani et al., 2012). Subsequent analysis and identification of candidate variants was performed with an in-house workflow incorporating the annotated variant data and pedigree information. Sanger sequencing verified candidate variants.

Two candidate compound heterozygous mutations were identified: a de novo single base pair deletion NM_015284.3:c.5499delC (p.Phe1834Serfs*47) predicted to result in premature protein truncation and a maternally inherited substitution at NM_015284.3: c.6916G > A (p.Gly2306Arg) (Table 1) (Vanderver et al., 2016). The p. Gly2306Arg missense variant is predicted to be “probably damaging” by PolyPhen-2 (score: 0.995) and “deleterious” by SIFT (score: 0.01) (Adzhubei et al., 2010; Cingolani et al., 2012; Kumar, Henikoff, & Ng,

2009). Both variants have a significant CADD score of 31 (Kircher et al., 2014). The p.Gly2306 residue is conserved in all vertebrate linages, as shown in Figure 1b. Neither variant has been reported in Genome Aggregation Database (gnomAD) or Leiden Open (source) Variation Database (LOVD).

5 | DISCUSSION

In this report, we describe a young girl with profound global developmental delay and regression, refractory epilepsy, and loss of central myelination, for whom WES identified novel mutations in the *SZT2* gene (Table 1). Falcone et al. (2013) reported a family with three macrocephalic children with mild-to-moderate intellectual disability without seizures and with normal brain imaging. Several additional case reports describe a more severe clinical phenotype associated with mutations in *SZT2,* similar to our patient (Basel-Vanagaite et al., 2013; Nakamura et al., 2017; Tshuchida et al., 2017; Venkatesan et al., 2016).

Previously reported MRI changes include a short, thick corpus callosum and migrational abnormalities (Table 1) (Basel-Vanagaite et al., 2013; Nakamura et al., 2017; Tshuchida et al., 2017; Venkatesan et al., 2016). Corpus callosum changes are common to many genetic epilepsy syndromes and disorders of brain development and were identified in most of the reported *SZT2* cases, including our own patient (Table 1) (Unterberger, Bauer, Walser, & Bauer, 2016). The patient in this report is similar to previous reports of the *SZT2*-related EOEE, but demonstrates unique imaging findings (Figure 1a and Table 1). The serial images obtained for our patient revealed normal myelination evolving into a progressive loss of typical development of myelination and worsening global atrophy (Figure 1a). The connection between *SZT2* and myelination is yet to be elucidated, although our patient demonstrates typical myelination until ~2 years of age, followed by a slow loss of normal T2/T1 weighted signal on neuroimaging. The loss of typical posterior pituitary signal, as found in our patient, can be clinically associated with SIADH (Papapostolou, Mantzoros, Evagelopoulou, Moses, & Kleefield, 1995). It is possible that the progressive atrophy is secondary to the refractory epilepsy rather than a direct effect from *SZT2.* In the future, electromyography and nerve conduction studies could be used to explore the role of *SZT2* in peripheral demyelination as well, as the loss of reflexes in our patient could be consistent with a peripheral neuropathy, a common feature among several leukodystrophies (Dali et al., 2015). One previously reported patient was noted to have diminished reflexes as well (Tshuchida et al., 2017).

In this case study, we describe an affected child with compound heterozygous variants in *SZT2* who presented with early-onset epileptic encephalopathy and progressive loss of typical development of myelination and atrophy on neuroimaging. Collectively, these reports demonstrate the emerging role of *SZT2* in epilepsy and cerebral function (Basel-Vanagaite et al., 2013; Falcone et al., 2013; Frankel et al., 2009; Peng et al., 2017; Tshuchida et al., 2017; Venkatesan et al., 2016). These cases underscore the broad phenotypic variability associated with *SZT2* mutations, ranging from mild intellectual disability to severe EOEE, as well as the breadth of potential imaging abnormalities, including myelination defects as demonstrated in this report.

ACKNOWLEDGMENTS

GH, AP, and AV are supported by the Myelin Disorders Bioregistry Project. GH is supported by the Delman Fund for Pediatric Neurology Education, RJT by an Australian Research Council Discovery Early Career Research Award. LA: Supported by grants from the CURE grant and the Lysosomal Disease Network. The Lysosomal Disease Network (U54NS065768) is a part of the Rare Diseases Clinical Research Network (RDCRN), an initiative of the Office of Rare Diseases Research (ORDR), and NCATS. This consortium is funded through collaboration between NCATS, the National Institute of Neurological Disorders and Stroke (NINDS), and the National Institute of Diabetes and Digestive and Kidney Diseases (NIDDK).

Funding information

Illumina, Gilead Sciences, Eli Lilly, Shire, Myelin Disorders Bioregistry Project, Delman Fund for Pediatric Neurology Education, Australian Research Council Discovery Early Career Research Award, CURE grant, Lysosomal Disease Network, Grant/Award Number: U54NS065768; NCATS, National Institute of Neurological Disorders and Stroke, National Institute of Diabetes and Digestive and Kidney Diseases

DISCLOSURE OF INTERESTS

A.V. receives funding and research support from Illumina, Gilead Sciences, Eli Lilly, and Shire. R.J.T. is an employee of Illumina.

REFERENCES

Adzhubei IA, Schmidt S, Peshkin L, Ramensky VE, Gerasimova A, Bork P, … Sunyaev SR (2010). A method and server for predicting damaging missense mutations. Nature Methods, 7(4), 248–249. 10.1038/nmeth0410-248 [PubMed: 20354512]

Baldassari S, Licchetta L, Tinuper P, Bisulli F, & Pippucci T (2016). GATOR1 complex: The common genetic actor in focal epilepsies. Journal of Medical Genetics, 53(8), 503–510. 10.1136/jmedgenet-2016-103883 [PubMed: 27208208]

Basel-Vanagaite L, Hershkovitz T, Heyman E, Raspall-Chaure M, Kakar N, Smirin-Yosef P, … Borck G (2013). Biallelic SZT2 mutations cause infantile encephalopathy with epilepsy and dysmorphic corpus callosum. American Journal of Human Genetics, 93(3), 524–529. 10.1016/j.ajhg.2013.07.005 [PubMed: 23932106]

Cingolani P, Platts A, Wang LL, Coon M, Nguyen T, Wang L, … Ruden DM (2012). A program for annotating and predicting the effects of single nucleotide polymorphisms, SnpEff: SNPs in the genome of Drosophila melanogaster strain w1118; iso-2; iso-3. Fly (Austin), 6(2), 80–92. 10.4161/fly.19695 [PubMed: 22728672]

Cleary JG, Braithwaite R, Gaastra K, Hilbush BS, Inglis S, Irvine SA, … De La Vega FM (2014). Joint variant and de novo mutation identification on pedigrees from high-throughput sequencing data. Journal of Computational Biology, 21(6), 405–419. 10.1089/cmb.2014.0029 [PubMed: 24874280]

Dali CÍ, Barton NW, Farah MH, Moldovan M, Månsson J-E, Nair N, … Krarup C (2015). Sulfatide levels correlate with severity of neuropathy in metachromatic leukodystrophy. Annals of Clinical and Translational Neurology, 2(5), 518–533. 10.1002/acn3.193 [PubMed: 26000324]

Falcone M, Yariz KO, Ross DB, Foster J 2nd, Menendez I, & Tekin M (2013). An amino acid deletion inSZT2 in a family with non-syndromic intellectual disability. PLoS One, 8(12), e82810. 10.1371/journal.pone.0082810 [PubMed: 24324832]

Frankel WN, Yang Y, Mahaffey CL, Beyer BJ, & O'Brien TP (2009). Szt2, a novel gene for seizure threshold in mice. Genes, Brain and Behavior, 8(5), 568–576. 10.1111/j.1601-183X.2009.00509.x

Kircher M, Witten DM, Jain P, O'Roak BJ, Cooper GM, & Shendure J (2014). A general framework for estimating the relative pathogenicity of human genetic variants. Nature Genetics, 46(3), 310–315. 10.1038/ng.2892 [PubMed: 24487276]

Kumar P, Henikoff S, & Ng PC (2009). Predicting the effects of coding non-synonymous variants on protein function using the SIFT algorithm. Nature Protocols, 4(7), 1073–1081. 10.1038/nprot.2009.86 [PubMed: 19561590]

Nakamura Y, Togawa Y, Okuno Y, Muramatsu H, Nakabayashi K, Kuroki Y, … Saitoh S (2017). Biallelic mutations in SZT2 cause a discernible clinical entity with epilepsy, developmental delay,

macrocephaly and a dysmorphic corpus callosum. Brain Development, 40, 134–139. 10.1016/j.braindev.2017.08.003 [PubMed: 28893434]

Papapostolou C, Mantzoros CS, Evagelopoulou C, Moses AC, & Kleefield J (1995). Imaging of the sella in the syndrome of inappropriate secretion of antidiuretic hormone. Journal of Internal Medicine, 237(2), 181–185. [PubMed: 7852921]

Peng M, Yin N, & Li MO (2017). SZT2 dictates GATOR control of mTORC1 signalling. Nature, 543(7645), 433–437. 10.1038/nature21378 [PubMed: 28199315]

Toutzaris D, Lewerenz J, Albrecht P, Jensen LT, Letz J, Geerts A, … Methner A (2010). A novel giant peroxisomal superoxide dismutase motif-containing protein. Free Radical Biology and Medicine, 48 (6), 811–820. 10.1016/j.freeradbiomed.2009.12.023 [PubMed: 20045724]

Tshuchida N, Nakashima M, Miyauchi A, Yoshitomi S, Kimizu T, Ganesan V, … Matsumoto N (2017). Novel biallelic SZT2 mutations in three cases of early-onset epileptic encephalopathy. Clinical Genetics, 93:266–274. 10.1111/cge.13061 [PubMed: 28556953]

Unterberger I, Bauer R, Walser G, & Bauer G (2016). Corpus callosum and epilepsies. Seizure, 37, 55–60. 10.1016/j.seizure.2016.02.012 [PubMed: 27010176]

Vanderver A, Simons C, Helman G, Crawford J, Wolf NI, Bernard G, … Taft RJ (2016). Whole exome sequencing in patients with white matter abnormalities. Annals of Neurology, 79(6), 1031–1037. 10.1002/ana.24650 [PubMed: 27159321]

Venkatesan C, Angle B, & Millichap JJ (2016). Early-life epileptic encephalopathy secondary to SZT2 pathogenic recessive variants. Epileptic Disorder, 18(2), 195–200. 10.1684/epd.2016.0828

Wolfson RL, Chantranupong L, Wyant GA, Gu X, Orozco JM, Shen K, … Sabatini DM (2017). KICSTOR recruits GATOR1 to the lysosome and is necessary for nutrients to regulate mTORC1. Nature, 543(7645), 438–442. 10.1038/nature21423 [PubMed: 28199306]

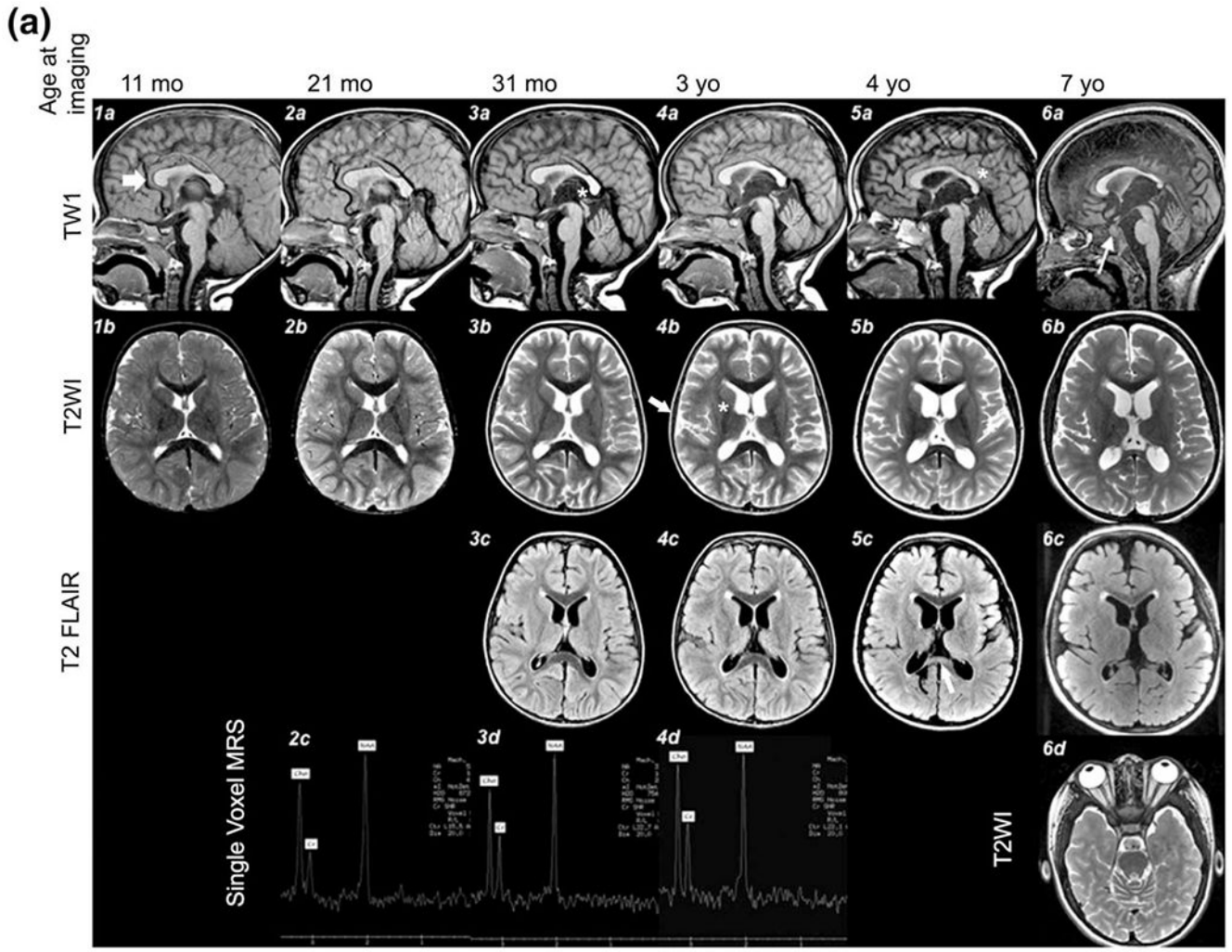

(b)

```
Homo sapiens (Human)                    VDSSSAQNGAPRLRLDVWEKGNISIVQLEEKLRGAARQALA
Mus musculus (Mouse)                    LDSCSAQDGSPRLRLDVWEKGNISIVQLEEKLRAAARQALA
Canis lupus familiaris (Dog)            SDSSSAQNGAPWLRLDVWEKGNISIVQLEEKLRGAARQALA
Bos taurus (Bovine)                     PGSSSAPSGAPRLRLDVWEKGNISIVQLEEKLRTAARQALA
Cavia porcellus (Guinea pig)            PDNSSAESGAPRLRLDVWEKGNISIVQLEEKLRGAARQALA
Gallus gallus (Chicken)                 AGT-QHTEPCVLVRLDIWEKGNISLLQLSEKLRGALRHALC
Alligator mississippiensis (Alligator)  PGM-LQPGPCARVRLDVWEKGNISLLQLSEKLRGALRHALC
Takifugu rubripes (Pufferfish)          SSS-SAAESKLFVRFDIWEQGNVSSLQLSDKLQGALRHALC
                                         .          :*:*:**:**:* :**.:**: * *:**.
```

FIGURE 1.

(a) Serial MRI of a patient with SZT2 mutations. (1) Imaging at 11 months demonstrates macroencephaly with mild generalized thickening of the corpus callosum. The blunted callosal rostrum is consistent with mild dysgenesis (white arrow, 1a). Myelination is normal. (2) Imaging at 21 months is unchanged with persistent megalencephaly, thickening of the corpus callosum, blunting of the rostrum, and normal myelination. Single voxel MR spectroscopy (MRS; TR 1500, TE 288) over the left basal ganglia reveals diminished creatine (Cr) with consequent elevation of Choline (Cho) to creatine and N-acetylaspartate

(NAA) to creatine ratios for age. (3) Images at 31 months show interval onset of mild diffuse brain volume loss with mild prominence of sulci and ventricles. The thalamic mass intermedia is absent (white asterisk, 3a). Myelin progression is less than expected for age, consistent with delayed or regression of myelination. Single voxel MR spectroscopy over the left basal ganglia shows an interval mild increase in Cr which remains mildly diminished with persistent elevation of Cho:Cr and NAA:Cr ratios for age. (4) Images at 3 years depict interval further diffuse brain volume loss with mild prominence of sulci (white arrow, 4b) and ventricles (white asterisk, 4b). The splenium is smaller in caliber than the genu and myelination has regressed. Single voxel MRS over the left basal ganglia shows interval normalization of Cr, NAA:Cr, and Cho:Cr ratios for age. (5) Images at 4 years show interval further diffuse brain volume loss with mild prominence of sulci and ventricles. The splenium has decreased further in size (asterisk, 5a), and is now abnormally bright (white arrow, 5c). Myelination continues to regress. The adenohypophysis is newly enlarged with maintenance of normal posterior pituitary signal. (6) Images at 7 years demonstrate interval further diffuse brain volume loss with prominence of sulci and ventricles, decreased splenium, and regression of myelination. The adenohypophysis has increased further in size with new loss of normal posterior pituitary signal (white arrow, 6a). The imaging shows hypertelorism with mild symmetric microphthalmia (6d). (b) Alignment of the SZT2 protein sequence surrounding the mutated residue p.Gly2306 (shown by arrow) to homologous SZT2 protein sequences from representative vertebrate species. SZT2 protein sequences were retrieved from uniprot and full-length protein alignments were generated with Clustal Omega

TABLE 1

Clinical and radiographic features of SZT2 pathogenic variants

Individual	*SZT2* mutation gene: protein	Mutation type	Clinical phenotype	Imaging findings by MRI
1 (Basel-Vanagaite et al., 2013)	c.73C>T: p.Arg25*	Homozygous	EOEE, dysmorphic features (high forehead, ptosis, downslanting palpebral fissures)	CC dysgenesis, peristent cavum septum pellucidum
2 (Basel-Vanagaite et al., 2013)	c,1496G>T: p.Ser499lle c.2092C>T:p.Gln698*	Compound heterozygous	EOEE, dysmorphic features (high forehead, ptosis, downslanting palpebral fissures)	CC dysgenesis, persistent cavum septum pellucidum
3 (Venkatesan et al., 2016)	c.3509_3512delCAGA: p.Thr1170ArgfsTer22 c.9703 C>T: p.Arg3235*	Compound heterozygous	EOEE, dysmorphic features (macrocephaly, downslanted palpebral fissures)	Migrational abnormalities
4–6 (siblings) (Falcone et al., 2013)	c.4202_4204delTTC: p.Phe1401del	Homozygous	Mild-moderate ID, macrocephaly	Normal
7 (Tshuchida et al., 2017)	c.3700_3716del: p.Asn1234Alafs*35 c.5482del: p.Gly1829Valfs*52	Compound heterozygous	EOEE, severe ID, dysmorphic features (high forehead, ptosis, arched eyebrows)	CC dysgenesis
8 (Tshuchida et al., 2017)	c.3947dup: p.Glu1317Glyfs*4 c.2929 + 1G>A: p.Leu939Aspfs*19	Compound heterozygous	EOEE, severe ID, high forehead	CC atrophy, persistent cavus septum pellucidum, enlarged ventricles
9 (Tshuchida et al., 2017)	c.7303C>T: p.Arg2435Trp c.8162C>G: p.Ser2721Cys	Compound heterozygous	EOEE, severe ID, Duane anomaly, high-arched palate, microcephaly	CC atrophy, enlarged ventricles
10 (Nakamura et al., 2017)	c.8596dup: p.Tyr2866Leufs*42 c.4181C>T: p.Pro1394Leu)andc.2930-17_2930-3delinsCTCGTG	Compound heterozygous	EOEE, moderate ID, macrocephaly, high forehead, hypertelorism	CC dysgenesis
11 (current patient)	c.5499delC: p.Phe1834Serfs*47 c.6916G>A: p.Gly2306Arg	Compound heterozygous	EOEE, dysmorphic features (macrocephaly with frontal bossing, flattened nasal bridge, hypertelorism)	CC dysgenesis, loss of myelination and progressive atrophy

Note.; * = stop codon; CC = corpus callosum; del = deletion; EOEE = early-onset epileptic encephalopathy; fs = frameshift; ID = intellectual disability.